

# Electrostatic effects influence the formation of two-dimensional crystals of bacteriorhodopsin reconstituted into dimyristoylphosphatidylcholine membranes

Received February 21, 2011; accepted March 21, 2011; published online April 9, 2011

Lumi Negishi\* and Shigeki Mitaku

Department of Applied Physics, Graduate School of Engineering,  
Nagoya University, Japan

\*Lumi Negishi, Department of Life Science, Graduate School of  
Bioscience and Biotechnology, Tokyo Institute of Technology,  
4259-B1, Nagatsuta-cho, Midori-ku, Yokohama, Kanagawa  
226-8501, Japan. Tel: +81-45-924-5825, Fax: +81-45-924-5807,  
email: lnegishi@bio.titech.ac.jp

We examined how electrostatic shielding affects the formation of two-dimensional (2D) crystals of bacteriorhodopsin (bR) in reconstituted dimyristoylphosphatidylcholine (DMPC) membranes by varying the sodium chloride (NaCl) concentration. The 2D crystalline array of bR formed in the gel phase of DMPC membranes was characterized by a symmetric bipolar pattern in visible circular dichroic spectra collected around 560 nm. The amplitude of the bipolar pattern was systematically enhanced by increasing the NaCl concentration. A strong correlation between the amplitude of the bipolar pattern and the Debye constant of small ions indicated that a weakening of electrostatic repulsion by the shielding effect of small ions enhances the order of 2D bR crystals in the gel phase of DMPC membranes. Considering the 3D distribution of charged residues, we propose a model of interaction balance in reconstituted bR membranes in which effective attraction between bR molecules occurs as a result of the phase separation of the DMPC membrane in the gel phase overcoming electrostatic repulsion between bR molecules.

**Keywords:** bacteriorhodopsin/circular dichroic spectrum/crystalline lattice/electrostatic repulsion/membrane protein.

**Abbreviations:** bR, bacteriorhodopsin; CD, circular dichroism; DMPC, dimyristoylphosphatidylcholine; NaCl, sodium chloride; 2D, two-dimensional.

Many membrane proteins form supramolecular complexes in which the configuration of the proteins involved is closely related to the function of complexes (1). Therefore, understanding the mechanism of membrane protein complex formation from both the physical and biological perspectives is very important. Bacteriorhodopsin (bR), a membrane protein that functions as a light driven proton pump, is an excellent

model for investigating the mechanisms of membrane protein complex formation, since bR molecules spontaneously form two-dimensional (2D) crystalline arrays known as purple membranes. Bacteriorhodopsin is the only protein component of purple membranes (2), and the basic information regarding the amino acid sequence (3, 4), the 3D structure (5–7), and the relationship between the photocycle and structural changes of bR molecules (8–10) is available. Bacteriorhodopsin reconstitution experiments are useful for elucidating the mechanism of bR crystallization because the 2D crystallization of bR in reconstituted membrane correlates well with the gel-to-liquid crystal transition of lipid bilayers (11). Previous studies of bR crystallization in reconstituted membranes may be classified into two categories: studies focusing on the effects of lipid bilayer phase transition (11–18), and observation of how the concentration of negatively charged lipids and salts influences 2D crystal formation (19–21).

Studies in the former category were carried out by several methods including visible circular dichroic (CD) spectroscopy (11, 12), X-ray diffraction (11), electron microscope (11, 12, 16) and rotational diffusion measurements (12, 13). Both spectroscopic measurements and the structural analyses indicate that bR molecules crystallized at the gel phase of lipid bilayer and melt at the liquid crystalline phase. The crystalline order of bR can be observed even at high temperature, when the protein concentration is so high that the lipid bilayer transition has vanished (20, 21). We recently investigated the correlation between the lipid membrane phase transition temperature and the crystallization temperature of bR, using three different neutral phospholipids: dimyristoyl-, dipalmitoyl- and distearoylphosphatidylcholine (18). Visible region CD spectra of bR reconstituted into these phospholipids demonstrated a bipolar pattern arising from the ordered configuration of bR below the lipid bilayer phase transition temperature. Collectively, these results indicated that the crystallization of bR in the lipid bilayer of synthetic neutral phospholipids is at least partly driven by effective attraction between bR molecules due to phase separation in the gel phase of lipid bilayer.

The contribution of negatively charged halo-lipids to the stability of the crystalline lattice in purple membranes suggests that other factors are involved in 2D crystallization of bR in reconstituted membranes. The 2D crystallization of bR in reconstituted membranes that are completely free of endogenous halo-lipids does

not occur under low ionic concentration, even below the lipid phase transition temperature (19–21). Furthermore, using reconstituted dimyristoylphosphatidylcholine (DMPC) membrane of delipidated bR with individual halo-lipids, Sternberg *et al.* (20) determined that the negatively charged polar groups of halo-lipids are essential for 2D crystallization of bR, while Krebs and Isenbarger extensively discussed the specific interaction between bR and lipid molecules in native purple membranes and that negatively charged halo-lipids contribute to the stability of the crystalline lattice in purple membranes (22–28). Sternberg *et al.* (20, 21) also clearly showed that a high concentration of salt in the solvent enhances the degree of crystallization of bR in reconstituted membranes. However, the effects of lipid bilayer phase separation and the electrostatic interaction between proteins and lipids have not been investigated in detail.

In this work, we employed a protein–lipid system to estimate the contribution of electrostatic interaction to the crystallization of bR in reconstituted DMPC membranes. By simply adding small ions to the aqueous reconstitution solvent, the electrostatic interactions were modified by the Debye shielding effect. We collected visible CD spectra of bR in reconstituted membranes with DMPC in the gel phase, varying the sodium chloride (NaCl) concentration. The bipolar pattern observed in visible CD spectra was significantly enhanced by increasing the NaCl concentration up to 1.0 M. Furthermore, a strong linear correlation between the intensity of the bipolar pattern and the Debye constant of the aqueous solvent was observed, indicating that electrostatic interactions between bR molecules have a tremendous influence on the formation of bR complexes in reconstituted membranes. Based on the amino acid sequence and 3D structure of bR, we hypothesize that the electrostatic interaction between bR molecules is repulsive in reconstituted DMPC membranes but attractive in purple membrane through negatively charged lipids.

## Materials and Methods

### Chemical reagents

DMPC was purchased from Avanti Polar Lipids, Inc. (Alabama, USA). Triton X-100 and other chemicals were purchased from Wako Pure Chemical Industries, Ltd. (Osaka, Japan). All materials were used without further purification.

### Preparation of purple membranes

Purple membranes of *Halobacterium salinarum*, strain R1M1, were isolated and purified according to the established method described by Oesterhelt and Stoecknius (29). Purified purple membranes were suspended in 100 mM Tris–HCl buffer (pH 7.0, 25°C) and sonicated for 5 min.

### Reconstitution of bR into DMPC vesicles

Reconstitution of bR into DMPC vesicles was carried out according to previously reported procedures (11, 13, 30, 31). Bacteriorhodopsin molecules were solubilized in 50 mM Triton X-100 at 25°C for 3 h in the dark. Solubilized bR was then mixed with a suspension of DMPC vesicles at a 1:150 protein:lipid molar ratio (50 μM bR:7.5 mM DMPC) and incubated at 30°C for 3 h in the dark, after which the suspension was dialysed against distilled water for 12 h at 29°C. The suspension was then dialysed for an additional week at 4°C in the dark, producing a transparent purple sample of

bR reconstituted into DMPC vesicles. We removed residual detergent by gently stirring the sample with Bio-Beads (SM2) (Bio-Rad Laboratories Inc., CA, USA) at room temperature at a concentration of 25 mg of beads per millilitre. We removed the beads by pipetting off the sample, yielding the final reconstituted bR-DMPC membrane product. Just before the measurements of circular dichroism spectra, we suspended the sample in a solution containing 100 mM Tris–HCl and NaCl at a final concentration between 0.0 and 1.0 M.

### Spectroscopic measurements

Absorption spectra of reconstituted bR-DMPC membranes were collected using a photo-diode array spectrophotometer with a thermostat cell holder (Agilent 8453, Agilent Technologies Inc., CA, USA). Reversibility, which is the ratio of stable bR after the incubation to before, was determined as follows: reconstituted bR solution was incubated for 1 h at 10–70°C in the dark to allow for thermal bleaching. This solution was then immediately cooled in ice water and the irreversible component spectral changes were determined from the ratio of the absorption of the quenched sample to that of the original sample before it was incubated at high temperature.

The crystallization of bR molecules in reconstituted vesicles was monitored by circular dichroism (CD) spectroscopy at a wavelength range between 400 and 700 nm in the dark, using a spectropolarimeter with a thermostat cell holder (J-820, JASCO, Tokyo, Japan). The protein concentration in the CD measurements was ~10 μM. To investigate the dependence of the degree of crystallization on the Debye constant, we collected CD spectra of reconstituted bR, varying the NaCl concentration (0, 0.1, 0.5 and 1.0 M) over a temperature range of 10–35°C, which covers the phase transition temperature of DMPC.

## Results

To explain the contribution of electrostatic interaction to 2D crystallization of bR in reconstituted membrane, we carried out three different experiments: (i) we measured the absorption spectra to determine whether bR molecules are denatured or not; (ii) we examined the temperature dependence of the visible CD spectra to determine the condition of the 2D crystallization of bR; and (iii) we evaluated the dependence of the visible CD spectra on the ionic concentration to elucidate the effect of electrostatic interaction on the 2D crystals of bR in the gel phase of the reconstituted membrane.

We first measured absorption spectra of reconstituted bR in NaCl free and 1.0 M NaCl buffers in the dark [Fig. 1A(a) and (b)] to determine the thermal stability of bR in the reconstituted membranes. Figure 1B shows the reversibility, which is the ratio of stable bR after the incubation to before, of reconstituted bR in NaCl free and 1.0 M NaCl buffers. Reconstituted bR in DMPC membranes destabilized above 60°C in the dark, irrespective of the presence of NaCl. These results indicated that at temperatures up to 60°C, the thermal stability of bR in DMPC membranes in the dark does not depend on the salt concentration.

We collected visible CD spectra of reconstituted bR in DMPC membranes over the temperature range of 10–35°C, covering the phase transition temperature of DMPC, which occurs at ~24°C (32, 33). Figure 2A shows the visible CD spectra of reconstituted bR-DMPC membranes at NaCl concentrations ranging from 0.0 to 1.0 M. Previous studies have established that a bipolar pattern in visible CD spectra is characteristic of the ordered configuration of bR, and

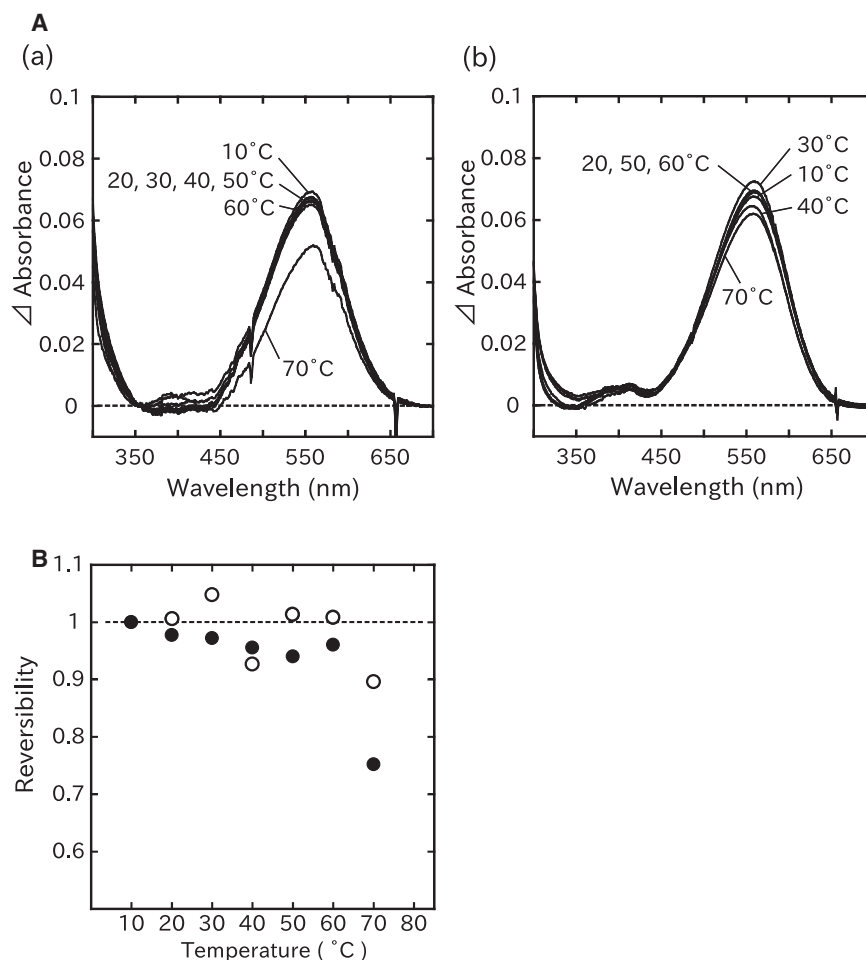


**Fig. 1** Salt effect on thermal stability of bR in the dark. (A) Absorption spectra of reconstituted bR in the dark in NaCl free (a) and 1.0 M NaCl buffer (b) after 1 h incubation at 10–70°C. The numbers in the graphs represent the temperature (°C). (B) The ratio of irreversible thermal bleaching of reconstituted bR in NaCl free (filled circles) and 1.0 M NaCl buffer (open circles) exhibiting same behavior of temperature dependence of the thermal denaturation.

that positive monopolar spectra represent the disordered configuration of bR (34–37). We found that CD spectra of bR in reconstituted membranes at 30°C are of the monopolar type irrespective of the NaCl concentration, indicating that the configuration of bR in reconstituted membranes is disordered because of lipid bilayer melting. On the other hand, CD spectra collected at 10°C showed a bipolar pattern, in which the amplitude differed depending on the NaCl concentration. The bipolar pattern was most pronounced at a NaCl concentration of 1.0 M, while CD spectra collected at lower NaCl concentrations appeared to be a combination of bipolar and monopolar spectra.

To estimate the amplitude of the bipolar pattern observed in visible CD spectra, we calculated differential spectra by subtracting the monopolar spectrum collected at 30°C from the spectra collected at other temperatures (Fig. 2B). The amplitude of the bipolar pattern of bR CD spectra determined from the difference between the maxima and minima are shown as a function of temperature in Fig. 3. The amplitude of the bipolar pattern started to rise just below the gel-to-liquid crystal transition of DMPC, ~24°C. The amplitude of the bipolar pattern increased steadily,

when the temperature was decreased to 10°C from the onset temperature of the ordered configuration. Although the tendency of the temperature dependence was the same among samples with different salt concentrations, the onset temperature as well as the amplitude at 10°C steadily increased as the NaCl concentration increased. The amplitude of the bipolar pattern in the sample with 1.0 M NaCl at 10°C was as large as that observed in native purple membrane CD spectra (38).

In order to better understand how ionic concentration impacts the amplitude of the bipolar pattern, we plotted the same data from Fig. 3 as a function of the Debye constant of solvents (Fig. 4). In this experiment, samples were buffered by 100 mM Tris–HCl; therefore, the Debye constant ( $K$ ) was calculated by adding 0.1 M to the NaCl concentration:

$$K = \sqrt{\frac{C_{\text{NaCl}} + C_{\text{buffer}}}{0.304}} \quad (1)$$

where  $C_{\text{NaCl}}$  and  $C_{\text{buffer}}$  represent the concentrations of the NaCl and Tris–HCl buffers, respectively. The NaCl concentration is represented by the upper abscissa in Fig. 4. The Debye constant is the inverse of

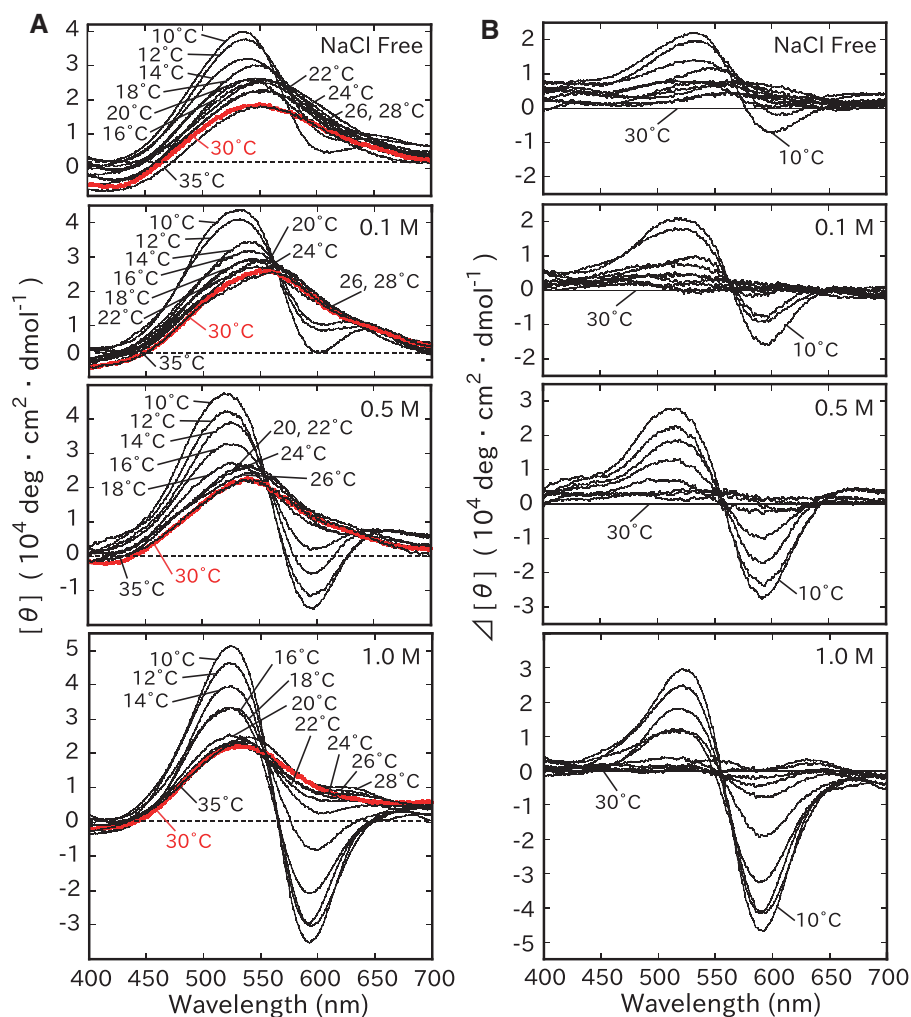


**Fig. 2** Salt concentration dependency of visible CD spectra. (A) CD spectra of bR reconstituted in DMPC membranes over a temperature range of 10–35°C in NaCl-free, 0.1 M NaCl, 0.5 M NaCl and 1.0 M NaCl. The numbers in the graph represent the temperature (°C). Red lines show spectra at 30°C. (B) Differences in the visible CD spectra of reconstituted bR membranes were obtained by subtracting the visible CD spectrum collected at 30°C from raw spectra collected at other temperatures in NaCl free, 0.1 M NaCl, 0.5 M NaCl and 1.0 M NaCl buffer.

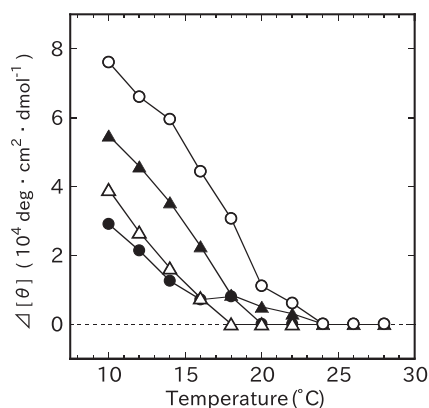


**Fig. 3** Difference between the maxima and minima of the bipolar patterns in plotted as a function of temperature in NaCl-free (filled circles), 0.1 M NaCl (open triangles), 0.5 M NaCl (filled triangles) and 1.0 M NaCl (open circles).

the Debye length, the characteristic length of the electrostatic shielding by ions in a solvent. These plots were fitted by linear regression, and the correlation coefficients ( $R^2$ ) were 0.99 for 10°C, 0.99 for 12°C,

0.98 for 14°C and 0.95 for 16°C. The bipolar part of the visible CD spectra was proportional to the Debye constant. The intercept of the linear relationship to the Debye constant of zero at 10°C was as small as  $1 \times 10^4 \text{ deg cm}^2 \text{ dmol}^{-1}$ , which was an order of magnitude smaller than the value obtained with a NaCl concentration of 1.0 M. This result indicated that the Debye shielding effect by small ions is an essential factor for crystallization of bR in reconstituted DMPC membranes, and that the contribution made by electrostatic interaction is contradictory to the effective attraction due to the lipid phase separation. We also conducted ionic concentration jump experiment. A jump in the NaCl concentration from 0.0 to 1.0 M led to a step-wise increase in the bipolar pattern of the CD spectra, corresponding to the shielding effect (data not shown).

## Discussion

Our results provide insight into three areas related to bR crystallization: the structural basis of the

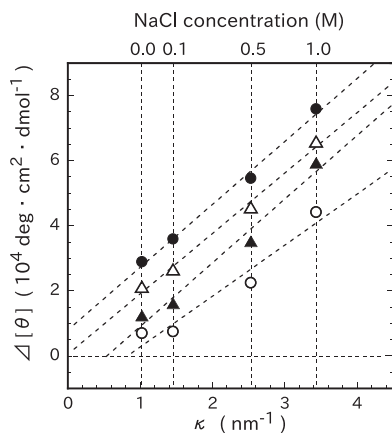


**Fig. 4** Amplitudes of the bipolar pattern of visible CD spectra collected at 10–16°C (filled circles, 10°C; open triangles, 12°C; filled triangles, 14°C; open circles, 16°C) plotted as a function of the Debye constant (the inverse of the Debye screening length). The small-ion concentration was increased by 0.1 M, corresponding to the concentration of Tris–HCl.

interaction balance between bR molecules in reconstituted membranes, the balance between the intermolecular interactions responsible for the crystallization of bR in the purple membrane, and the physiological meaning of the 2D crystallization of bR. The good correlation between the melting temperature of 2D bR crystals and the gel-to-liquid crystal phase transition temperature (11, 12, 18) indicates that the intermolecular interaction responsible for 2D crystallization of bR in reconstituted membranes is due to effective attraction brought about by the phase separation of lipid hydrocarbon chains. It is well known that van der Waals interactions between hydrocarbon chains give rise to the lipid membrane phase transition as well as the separation of other molecules in the gel phase, where lipid molecule hydrocarbon chains are tightly packed (39–42). The effective attraction due to the separation of bR molecules in the gel phase of DMPC vesicles is considered to be the motive force for crystallization of bR in reconstituted membranes. However, Sternberg *et al.* (19) reported that when halo-lipids are completely removed, no crystallization of bR is observed in the reconstituted membrane. The difference between our present work and that of Sternberg *et al.* is that the ionic concentration was much lower in their samples. The apparent discrepancy may be explained by differences in the degree of electrostatic shielding. In fact, Sternberg *et al.* (20) also reported 2D hexagonal crystal formation in reconstituted bR membranes with specific halo-lipids in solutions containing 4 M NaCl. As shown in Fig. 4, the degree of the crystallization at the gel phase of the lipid bilayer becomes very low when the ionic concentration is also very low. Since we measured systematic changes in the degree of the crystallization, we can discuss about the trace of the crystallization of samples in highly shielded solvent. Therefore, it is plausible that the weak crystallization of bR observed in samples with a low ionic concentration was incorrectly assumed to be due to the exchange of lipids (19, 20).

Our results indicate that changes in the small-ion concentration have a tremendous influence on the degree and order of bR crystallization. The bipolar pattern observed in visible CD spectra, which is an indication of an ordered configuration of bR molecules, was significantly enhanced with increasing NaCl concentration at 10°C, a temperature that is far below the point of gel-liquid crystal phase transition. The strong linear relationship we observed between the amplitude of the bipolar pattern and the Debye constant indicate that electrostatic interactions play an essential role in this system. Furthermore, since the crystalline order was enhanced due to electrostatic shielding, the electrostatic interaction in the reconstituted membrane system must be repulsive. This possible balancing of the electrostatic interactions with effective attraction due to lipid phase separation would explain the dependence of bR 2D crystallization in reconstituted membranes on the concentration of NaCl.

A conceptual experiment involving exchange of neutral DMPC lipids for negatively charged halo-lipids may clarify the mechanism imparting high stability upon the bR 2D crystal in purple membranes. The positively charged amino acids of bR molecules may form electric bridging with negatively charged head groups of halo-lipids. The position of bR amino acids in purple membrane with respect to the membrane are illustrated in Fig. 5A. The shaded regions in Fig. 5A represent the interface between the hydrophobic region of the membrane and water, which corresponds to the position of lipid head groups. This schematic was obtained by modifying the structural model reported by Mitsuoka *et al.* (28) and the amino acid sequence of bR obtained from Swiss-Prot (P02945 BACR\_HALSA). The interface regions of the membrane in the original model by Mitsuoka *et al.* were expanded by three residues. The number of charged amino acids is large, particularly on the cytoplasmic side of the molecule, and the charge distribution is biased, with more negative charge in the cytoplasmic aqueous phase and more positive charge in the cytoplasmic interface. The number of charged residues in the cytoplasmic interface did not change so much with that reported in an alternative definition of the interface region of bR (43). Thus, positively charged amino acids at the interface between the hydrophobic region and water can act as the counter-part to the negative charge of lipids. In fact, structural analyses of bR have demonstrated specific binding between a positively charged amino acid and a lipid molecule (26–28). Grigorieff *et al.* (44) suggested from the electron diffraction measurements that the orientation and distance between bR trimers in the 2D crystalline array is influenced by strong long-range electrostatic interactions. Figure 5B shows molecular structure image of the cytoplasmic interface region of bR (PDB ID; 1M0L) (45) produced using Discovery Studio Visualizer (Accelrys, Inc., CA, USA) (Fig. 5B). Analysis of the molecular structure of the bR cytoplasmic interface region shows that positively charged amino acids are concentrated in this region. Because the net charge of DMPC molecules is neutral, the

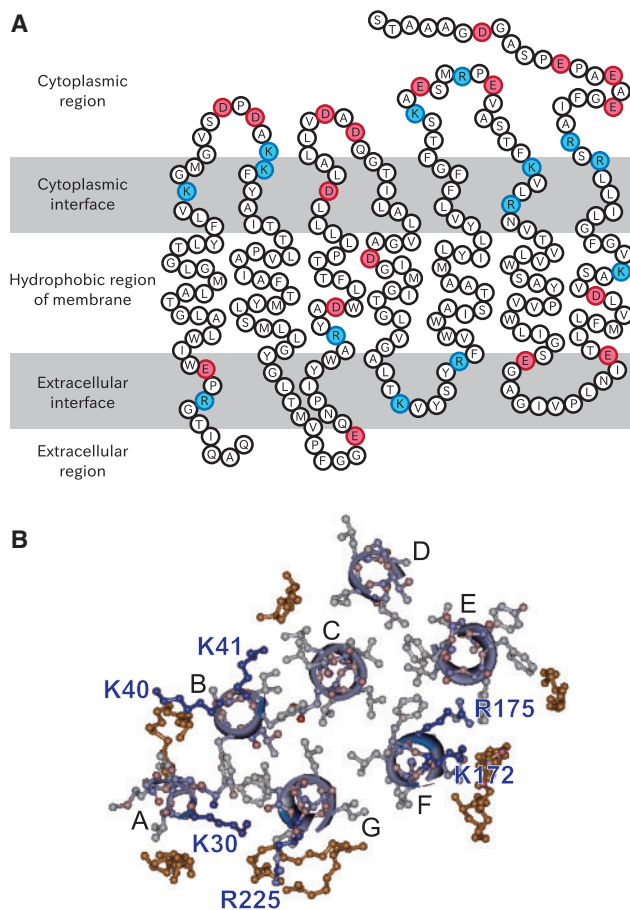


**Fig. 5 Charged amino acids distribution of bR in purple membrane.** (A) Schematic diagram of the bR amino acid sequence arranged topologically with respect to the membrane, based on the model described by Mitsuoka *et al.* (28). Membrane interface regions are shaded. Acidic amino acids are shown in red and basic amino acids are shown in blue. (B) Molecular structure of the cytoplasmic interface region of bR (PDB ID: 1M0L) (45) in which positively charged amino acids are concentrated. Image produced using Discovery Studio Visualizer (Accelrys, Inc., CA, USA).

characteristics of DMPC membrane such as the phase transition are almost independent of ionic concentration in solvents (46–48). The repulsion between positively charged amino acids probably hindered the 2D crystallization of bR in the reconstituted membranes while halo-lipid head groups with negative net charges can form bridges with the positively charged amino acids in the interface regions of bR in purple membranes. The high stability of the 2D crystals of bR in purple membranes can thus be explained by electrostatic attraction.

The model we present regarding the mechanism of bR 2D crystallization in purple membranes also suggests its biological significance. When positively charged amino acids located at the membrane–water interface are neutralized by negatively charged lipids, the negative charge density on the cytoplasmic side of bR crystals becomes very large, leading to an anomalously low pH (high proton concentration) at the cytoplasmic surface of the membrane. There is a possibility that elevated proton concentration is advantageous for

halo-bacteria because it accelerates the proton pumping function associated with bR and the purple membrane.

#### Funding

Grant-in-Aid for Scientific research from the Ministry of Education, Culture, Sports, Science and Technology of Japan; SENTAN from Japan Science and Technology Agency.

#### Conflict of interest

None declared.

#### References

- Gennis, R.B. (1988) *Biomembrane: Molecular Structure and Function*, Springer, New York
- Henderson, R. and Unwin, P.N.T. (1975) Three-dimensional model of purple membrane obtained by electron microscopy. *Nature* **257**, 28–32
- Khorana, H.G., Gerber, G.E., Herlihy, W.C., Gray, C.P., Anderegg, R.J., Nihei, K., and Biemann, K. (1979) Amino acid sequence of bacteriorhodopsin. *Proc. Natl. Acad. Sci. USA* **76**, 5046–5050
- Dunn, R., McCoy, J., Simsek, M., Majumdar, A., Chang, S.H., Rajbhandary, U.L., and Khorana, H.G. (1981) The bacteriorhodopsin gene. *Proc. Natl. Acad. Sci. USA* **78**, 6744–6748
- Grigorieff, N., Ceska, T.A., Downing, K.H., Baldwin, J.M., and Henderson, R. (1996) Electron-crystallographic refinement of the structure of bacteriorhodopsin. *J. Mol. Biol.* **259**, 393–421
- Kimura, Y., Vassilyev, D.G., Miyazawa, A., Kidera, A., Matsushima, M., Mitsuoka, K., Murata, K., Hirai, T., and Fujiyoshi, Y. (1997) Surface of bacteriorhodopsin revealed by high-resolution electron crystallography. *Nature* **389**, 206–211
- Luecke, H., Schobert, B., Richter, H.T., Cartailler, J.P., and Lanyi, J.K. (1999) Structure of bacteriorhodopsin at 1.55 Å resolution. *J. Mol. Biol.* **291**, 899–911
- Lozier, R.H., Bogomolni, R.A., and Stoekenius, W. (1975) Bacteriorhodopsin: a light-driven proton pump in *Halobacterium halobium*. *Biophys. J.* **15**, 955–962
- Lanyi, J.K. (1993) Proton translocation mechanism and energetics in the light-driven pump bacteriorhodopsin. *Biochim. Biophys. Acta* **1183**, 241–261
- Luecke, H. (2000) Atomic resolution structures of bacteriorhodopsin photocycle intermediates: the role of discrete water molecules in the function of this light-driven ion pump. *Biochim. Biophys. Acta* **1460**, 133–156
- Cherry, R.J., Müller, U., Henderson, R., and Heyn, M.P. (1978) Temperature-dependent aggregation of bacteriorhodopsin in dipalmitoyl- and dimyristoylphosphatidylcholine vesicles. *J. Mol. Biol.* **121**, 283–298
- Cherry, R.J., Müller, U., Hostenstein, C., and Heyn, M.P. (1980) Lateral segregation of proteins induced by cholesterol in bacteriorhodopsin-phospholipid vesicles. *Biochim. Biophys. Acta* **596**, 145–151
- Heyn, M.P., Cherry, R.J., and Dencher, N.A. (1981) Lipid-protein interactions in bacteriorhodopsin-dimyristoylphosphatidylcholine vesicles. *Biochemistry* **20**, 840–849
- Heyn, M.P., Blume, A., Rehorek, M., and Dencher, N.A. (1981) Calorimetric and fluorescence depolarization studies on the lipid phase transition of bacteriorhodopsin-dimyristoylphosphatidylcholine vesicles. *Biochemistry* **20**, 7109–7115

15. Lewis, B.A. and Engelman, D.M. (1983) Bacteriorhodopsin remains dispersed in fluid phospholipid bilayers over a wide range of bilayer thicknesses. *J. Mol. Biol.* **166**, 203–210
16. Gulik-Krzywicki, T., Seigneuret, M., and Rigaud, J.L. (1987) Monomer-oligomer equilibrium of bacteriorhodopsin in reconstituted proteoliposomes. A freeze-fracture electron microscope study. *J. Biol. Chem.* **262**, 15580–15588
17. Piknová, B., Pérochon, E., and Tocanne, J.F. (1993) Hydrophobic mismatch and long-range protein/lipid interactions in bacteriorhodopsin/phosphatidylcholine vesicles. *Eur. J. Biochem.* **218**, 385–396
18. Yokoyama, Y., Negishi, L., Kitoh, T., Sonoyama, M., Asami, Y., and Mitaku, S. (2010) Effect of lipid phase transition on molecular assembly and structural stability of bacteriorhodopsin reconstituted into phosphatidylcholine liposomes with different acyl-chain lengths. *J. Phys. Chem. B* **114**, 15706–15711
19. Sternberg, B., Gale, P., and Watts, A. (1989) The effect of temperature and protein content on the dispersive properties of bacteriorhodopsin from *H. halobium* in reconstituted DMPC complexes free of endogenous purple membrane lipids: A freeze-fracture electron microscopy study. *Biochim. Biophys. Acta.* **980**, 117–126
20. Sternberg, B., L'Hostis, C., Whiteway, C.A., and Watts, A. (1992) The essential role of specific *Halobacterium halobium* polar lipids in 2D-array formation of bacteriorhodopsin. *Biochim. Biophys. Acta.* **1108**, 21–30
21. Sternberg, B., Watts, A., and Cejka, Z. (1993) Lipid-induced modulation of the protein packing in two-dimensional crystals of bacteriorhodopsin. *J. Struct. Biol.* **110**, 196–204
22. Krebs, M.P. and Isenbarger, T.A. (2000) Structural determinants of purple membrane assembly. *Biochim. Biophys. Acta.* **1460**, 15–26
23. Kushwaha, S.C., Kates, M., and Martin, W.G. (1975) Characterization and composition of the purple and red membrane from *Halobacterium cutirubrum*. *Can. J. Biochem.* **53**, 284–292
24. Kates, M., Kushwaha, S.C., and Sprott, G.D. (1982) Lipids of purple membrane from extreme halophiles and of methanogenic bacteria. *Methods Enzymol.* **88**, 98–111
25. Joshi, M.K., Dracheva, S., Mukhopadhyay, A.K., Bose, S., and Hendler, R.W. (1998) Importance of specific native lipids in controlling the photocycle of bacteriorhodopsin. *Biochemistry* **37**, 14463–14470
26. Essen, L., Siegert, R., Lehmann, W.D., and Oesterhelt, D. (1998) Lipid patches in membrane protein oligomers: crystal structure of the bacteriorhodopsin-lipid complex. *Proc. Natl. Acad. Sci. USA* **95**, 11673–11678
27. Sato, H., Takeda, K., Tani, K., Hino, T., Okada, T., Nakasako, M., Kamiya, N., and Kouyama, T. (1999) Specific lipid-protein interactions in a novel honeycomb lattice structure of bacteriorhodopsin. *Acta Crystallogr. D Biol. Crystallogr.* **55 (Pt 7)**, 1251–1256
28. Mitsuoka, K., Hirai, T., Murata, K., Miyazawa, A., Kidera, A., Kimura, Y., and Fujiyoshi, Y. (1999) The structure of bacteriorhodopsin at 3.0 Å resolution based on electron crystallography: implication of the charge distribution. *J. Mol. Biol.* **286**, 861–882
29. Oesterhelt, D. and Stoekenius, W. (1974) Isolation of the cell membrane of *Halobacterium halobium* and its fractionation into red and purple membrane. *Methods Enzymol.* **31 (Pt A)**, 667–678
30. Heyn, M.P. and Dencher, N.A. (1982) Reconstitution of monomeric bacteriorhodopsin into phospholipid vesicles. *Methods Enzymol.* **88**, 31–35
31. Lévy, D., Bluzat, A., Seigneuret, M., and Rigaud, J.L. (1990) A systematic study of liposome and proteoliposome reconstitution involving Bio-Bead-mediated Triton X-100 removal. *Biochim. Biophys. Acta* **1025**, 179–190
32. Ladbroke, B.D. and Chapman, D. (1969) Thermal analysis of lipids, proteins and biological membranes. A review and summary of some recent studies. *Chem. Phys. Lipids* **3**, 304–367
33. Cronan, J.E. Jr and Gelmann, E.P. (1975) Physical properties of membrane lipids: Biological relevance and regulation. *Bacteriol. Rev.* **39**, 232–256
34. Bauer, P.J., Dencher, N.A., and Heyn, M.P. (1976) Evidence for chromophore-chromophore interactions in the purple membrane from reconstitution experiments of the chromophore-free membrane. *Biophys. Struct. Mech.* **2**, 79–92
35. Muccio, D.D. and Cassim, J.Y. (1979) Interpretation of the absorption and circular dichroic spectra of oriented purple membrane films. *Biophys. J.* **26**, 427–440
36. Wu, S. and El-Sayed, M.A. (1991) CD spectrum of bacteriorhodopsin: best evidence against exciton model. *Biophys. J.* **60**, 190–197
37. Cassim, J.Y. (1992) Unique biphasic band shape of the visible circular dichroism of bacteriorhodopsin in purple membrane: excitons, multiple transitions or protein heterogeneity? *Biophys. J.* **63**, 1432–1442
38. Yokoyama, Y., Sonoyama, M., and Mitaku, S. (2002) Irreversible photobleaching of bacteriorhodopsin in a high-temperature intermediate state. *J. Biochem.* **131**, 785–790
39. Höchli, M. and Hackenbrock, C.R. (1976) Fluidity in mitochondrial membranes: thermotropic lateral translational motion of intramembrane particles. *Proc. Natl. Acad. Sci. USA* **73**, 1636–1640
40. Kleemann, W. and McConnell, H.M. (1976) Interactions of proteins and cholesterol with lipids in bilayer membranes. *Biochim. Biophys. Acta* **419**, 206–222
41. Benga, G. and Holmes, R.P. (1984) Interactions between components in biological membranes and their implications for membrane function. *Prog. Biophys. Mol. Biol.* **43**, 195–257
42. Quinn, P.J. (1985) A lipid-phase separation model of low-temperature damage to biological membranes. *Cryobiology* **22**, 128–146
43. Saitô, H., Tsuchida, T., Ogawa, K., Arakawa, T., Yamaguchi, S., and Tuzi, S. (2002) Residue-specific millisecond to microsecond fluctuations in bacteriorhodopsin induced by disrupted or disorganized two-dimensional crystalline lattice, through modified lipid-helix and helix-helix interactions, as revealed by <sup>13</sup>C NMR. *Biochim. Biophys. Acta* **1565**, 97–106
44. Grigorieff, N., Beckmann, E., and Zemlin, F. (1995) Lipid location in deoxycholate-treated purple membrane at 2.6 Å. *J. Mol. Biol.* **254**, 404–415
45. Schobert, B., Cupp-Vickery, J., Hornak, V., Smith, S., and Lanyi, J. (2002) Crystallographic structure of the K intermediate of bacteriorhodopsin: conservation of free energy after photoisomerization of the retinal. *J. Mol. Biol.* **321**, 715–726
46. Träuble, H. and Eibl, H. (1974) Electrostatic effects on lipid phase transitions: membrane structure and ionic environment. *Proc. Natl. Acad. Sci. USA* **71**, 214–219
47. Cevc, G. (1991) Polymorphism of the bilayer membranes in the ordered phase and the molecular origin of the lipid pretransition and rippled lamellae. *Biochim. Biophys. Acta.* **1062**, 59–69
48. Koynova, R. and Caffrey, M. (1998) Phases and phase transitions of the phosphatidylcholines. *Biochim. Biophys. Acta* **1376**, 91–145